FINITE DIFFERENCE APPROXIMATIONS TO THE DIFFUSION EQUATION

1. Introduction

In the study of atmospheric motions within the Planetary Boundary Layer (PBL) a theory often employed to represent the sub grid scale turbulent transfer is that of eddy (or Reynold) stresses. Basically the idea is to separate the mean (time averaged) and instantaneous flows in the equation of motion. If U represents a mean component of velocity, then the equation for U has an added forcing term

$$K_m \frac{\partial^2 U}{\partial z^2} \qquad \ldots\ldots\ldots(1)$$

to account for fluctuations in the motion about the mean. Here K_m is assumed constant in the simplest form of the theory, and is termed the "eddy exchange coefficient for momentum".

In modelling the PBL numerically an uneven vertical grid spacing is frequently required with the lowest levels closest together. Since there is also a need for as large a time step in the numerical integration of the equations as possible, we require a stable scheme which can handle the diffusion terms (1) while remaining relatively insensitive to the value of Δz (the vertical grid spacing) throughout the PBL. The following notes describe the merits and disadvantages of schemes in this respect.

2. Finite Difference Approximations to

$$\frac{\partial v}{\partial t} = \sigma \frac{\partial^2 v}{\partial x^2} \qquad \sigma \text{ constant} > 0$$

(taken from Difference Methods for Initial-Value Problems by Richtmyer and Morton).

We summarise, in the following table, the various finite differences approximations to

$$\frac{\partial v}{\partial t} = \sigma \frac{\partial^2 v}{\partial x^2}, \qquad \ldots\ldots\ldots (2)$$

discussed in section 3. The mnenonic diagram at the left indicates the type of differencing employed. The points shown are those points in the x-t plane used in one application of the formula. The t - axis points to the top of the page and the x - axis horizontally to the right. Points connected horizontally are used in forming space differences. Those connected vertically are used in forming the time difference. The various

weights associated with sets of points are shown accordingly.

1.

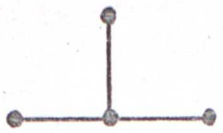

$$U_j^{n+1} - U_j^n = \lambda (\delta^2 U)_j^n$$

error = $O(\Delta t) + O[(\Delta x)^2]$

explicit, stable if λ = const. $\leq \frac{1}{2}$ as $\Delta t, \Delta x \to 0$.

(special case of 5 with $\theta = 0$)

2.

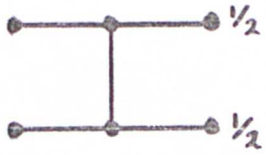

$$U_j^{n+1} - U_j^n = \lambda \left\{ (\delta^2 U)_j^n + (\delta^2 U)_j^{n+1} \right\} / 2$$

Crank & Nicholson (1947)

error = $O[(\Delta t)^2] + O[(\Delta x)^2]$

implicit, always stable.

(special case of 5 with $\theta = \frac{1}{2}$)

3.

$$U_j^{n+1} - U_j^n = \lambda (\delta^2 U)_j^{n+1}$$

error = $O(\Delta t) + O[(\Delta x)^2]$

implicit, always stable.

(special case of 5 with $\theta = 1$)

4.

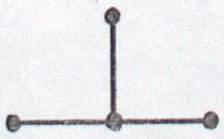

As 1, but with $\lambda = 1/6$

error = $O[(\Delta t)^2] + O[(\Delta x)^4]$

(special case of 1, stable.)

5.

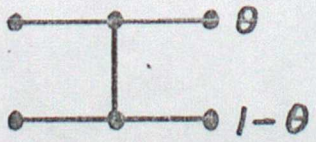

$$U_j^{n+1} - U_j^n = \lambda \left\{ \theta (\delta^2 U)_j^{n+1} + (1-\theta)(\delta^2 U)_j^n \right\}$$

where θ = const. $0 \leq \theta \leq 1$

error = $O(\Delta t) + O[(\Delta x)^2]$

for $0 \leq \theta < \frac{1}{2}$ stable if

λ = const. $\leq \frac{1}{2-4\theta}$;

for $\frac{1}{2} \leq \theta \leq 1$, always stable.

6. 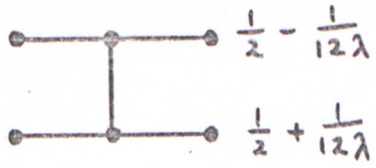

Same as 5 but with

$$\theta = \tfrac{1}{2} - \tfrac{1}{12\lambda}$$

error = $O[(\Delta t)^2] + O[(\Delta x)^4]$

stable.

7. 

$$U_j^{n+1} - U_j^{n-1} = \lambda\,(\delta^2 U)_j^n$$

always unstable.

8. 

$$U_j^{n+1} - U_j^{n-1} = \lambda\left\{ U_{j+1}^n - U_j^{n+1} - U_j^{n-1} + U_{j-1}^n \right\}$$

where $\frac{\Delta t}{\Delta x} \to 0$ as Δt, $\Delta x \to 0$

error = $O[(\Delta t)^2] + O[(\Delta x)^2] + O\left[\left(\frac{\Delta t}{\Delta x}\right)^2\right]$

Du Fort & Frankel (1953)

explicit always stable.

9. 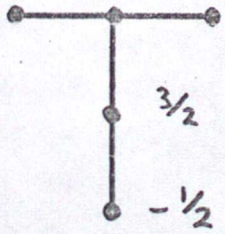

$$\tfrac{3}{2}\left(U_j^{n+1} - U_j^n\right) - \tfrac{1}{2}\left(U_j^n - U_j^{n-1}\right) = \lambda\,(\delta^2 U)_j^{n+1}$$

implicit, always stable.

(special case of 10 with $\theta = \frac{1}{2}$)

10. 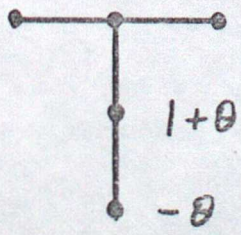

$$(1+\theta)\left(U_j^{n+1} - U_j^n\right) - \theta\left(U_j^n - U_j^{n-1}\right) = \lambda\,(\delta^2 U)_j^{n+1}$$

θ = const. > 0. λ = const > 0

implicit, always stable.

error = $O(\Delta t) + O[(\Delta x)^2]$.

11.

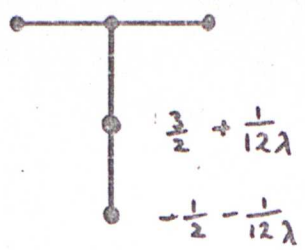

Same as 10, but with

$$\theta = \tfrac{1}{2} + \tfrac{1}{(12\lambda)}.$$

error $= O[(\Delta t)^2] = O[(\Delta x)^4]$

always stable.

12.

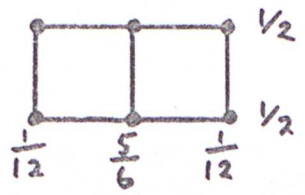

$$\tfrac{1}{12}\left\{U^{n+1}_{j+1} - U^{n}_{j+1}\right\} + \tfrac{5}{6}\left\{U^{n+1}_{j} - U^{n}_{j}\right\}$$
$$+ \tfrac{1}{12}\left\{U^{n+1}_{j-1} - U^{n}_{j-1}\right\} = \lambda\left\{(\delta^2 U)^{n+1}_{j} + (\delta^2 U)^{n}_{j}\right\}/2.$$

error $= O[(\Delta t)^2] + O[(\Delta x)^4]$

always stable; identical with scheme 6.

13.

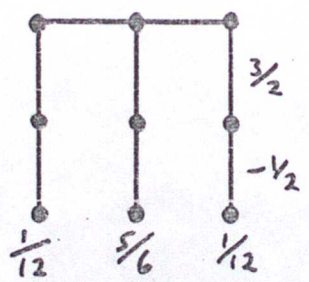

$$\tfrac{1}{12}\left\{\tfrac{3}{2}U^{n+1}_{j+1} - 2U^{n}_{j+1} + \tfrac{1}{2}U^{n-1}_{j+1}\right\}$$
$$+\tfrac{5}{6}\left\{\tfrac{3}{2}U^{n+1}_{j} - 2U^{n}_{j} + \tfrac{1}{2}U^{n-1}_{j}\right\}$$
$$+\tfrac{1}{12}\left\{\tfrac{3}{2}U^{n+1}_{j-1} - 2U^{n}_{j-1} + \tfrac{1}{2}U^{n-1}_{j-1}\right\}$$
$$= \lambda(\delta^2 U)^{n+1}_{j}$$

error $= O[(\Delta t)^2] + O[(\Delta x)^4]$

always stable.

14.

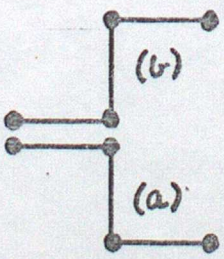

a) $U^{n+1}_{j} - U^{n}_{j} = \lambda\left(U^{n}_{j+1} - U^{n}_{j} - U^{n+1}_{j} - U^{n+1}_{j-1}\right)$

b) $U^{n+2}_{j} - U^{n+1}_{j} = \lambda\left(U^{n+2}_{j+1} - U^{n+2}_{j} - U^{n+1}_{j} - U^{n+1}_{j-1}\right)$

Saulev (1957)

Unconditionally stable.

3. Numerical Schemes

The various schemes discussed below are those summarised in the table in section 2.

If $f(x)$ is any function of x, we denote by δf_j or $(\delta f)_j$ the central difference

$$f((j+\tfrac{1}{2})\Delta x) - f((j-\tfrac{1}{2})\Delta x),$$

where j may be any integer. Hence $(\delta^2 f)_j$ represents the quantity

$$f((j+1)\Delta x) - 2f(j\Delta x) + f((j-1)\Delta x). \qquad \ldots\ldots(3)$$

If f depends on t, that dependence may be indicated by a superscript n. With this notation we wish to consider first the difference scheme (scheme 5)

$$U_j^{n+1} - U_j^n = \lambda\left\{\theta(\delta^2 U)_j^{n+1} + (1-\theta)(\delta^2 U)_j^n\right\}. \qquad \ldots\ldots(4)$$

θ is a real constant, generally thought of as lying between 0 and 1;
λ represents the constant $\sigma\Delta t/(\Delta x)^2$ and Δt the time interval.
Schemes 1 to 4 are special cases (4) with the appropriate choice of θ.

To discuss the stability of (4) we substitute the wavelike expression $\xi^n e^{ikj\Delta x}$ in place of U_j^n into (4). Cancelling multiplying factors we arrive at a growth factor ξ given by

$$\xi = \frac{1 - \lambda(1-\theta)x'}{1 + \lambda\theta x'}, \qquad \ldots\ldots(5)$$

where $k\Delta x = \alpha$ and $x' = 4\sin^2\frac{\alpha}{2}$.

It is sufficient, in this discussion, to limit ourselves to one harmonic of the above form, since any general solution of (4) or (2) may be built up from a linear superposition of such modes.

The analytic solution of (2) for a wave of the form e^{ikx} is

$$U = U_0 e^{-\sigma k^2 t}\cdot e^{ikx}. \qquad \ldots\ldots(6)$$

So the appropriate growth factor is $e^{-\sigma k^2\Delta t}$ where $n\Delta t = t$. Since $k\Delta x = \alpha$ and $\lambda = \sigma\Delta t/(\Delta x)^2$, this may be written as $e^{-\lambda\alpha^2}$. We have tabulated values of $\varepsilon\ (= \xi/e^{-\alpha^2\lambda})$ for various

values of α, λ and θ and exhibited the results in graphical form.

The smallest wavelength that can be resolved on a grid of length Δx is $2\Delta x$. Now the wavenumber k is related to the wavelength (L) by

$$k = 2\pi/L .$$

So with $\infty > L \geq 2\Delta x$ the range of α is $0 < \alpha \leq \pi$.

For stability of the solutions of (4) we require the growth factor ξ (given by (5)) to satisfy the condition

$$|\xi| \leq 1. \qquad \ldots\ldots(7)$$

If this condition is satisfied, the harmonic is not amplified at all, whereas if it is violated, the harmonic increases without limit - clearly physically unacceptable. From (5) we can show the condition (7) is satisfied under the following conditions:

Case i) $0 \leq \theta < 1/2$.
Stable provided $0 \leq \lambda \leq \frac{1}{2-4\theta}$

Case ii) $1 \geq \theta \geq 1/2$.
Always stable.

In figures 1-11 we have plotted values of ε against α for various values of λ, and θ ranging from 0 to 1 in steps of 0.1. Values of ε greater than one indicate that the numerical solution decays at a rate slower than the analytic one and vice versa. Values of one point to exact agreement between numerical and analytic solutions. $\varepsilon < 0$ indicates the finite difference approximation changes sign every time step, such cases being physically inconsistent with the analytic solution.

In each figure λ is a variable parameter giving a different curve for each ε, α plot. Of interest are curves which give positive ε for all values of α. As can be seen, all curves tend towards $\varepsilon = 1$ for long wavelength modes ($\alpha \approx 0$), but diverge widely for the short wavelengths ($\alpha \approx \pi$). Ideally we require the curves to cluster close to the line $\varepsilon = 1$ for as many values of λ (ie of Δx) as possible. For low values of θ, generally, the lines lie below $\varepsilon = 1$ while the reverse is true for values of θ greater than 0.4. The best scheme here to handle harmonic modes would appear to be that with $\theta = 0$ and $0 \leq \lambda \leq 0.25$. To

increase the range of λ , θ has to be increased appropriately, but the curves, in turn, diverge more from $\varepsilon = 1$ so losing any advantage gained.

The truncation error for scheme 5 (equation (4)) can be found quite easily to be

$$\text{error} = O(\Delta t) + O[(\Delta x)^2].$$

Scheme 6

This is just a special case of scheme 5 with

$$\theta = \tfrac{1}{2} - \tfrac{1}{12}\lambda \qquad \ldots\ldots(8)$$

This special value of θ has the effect of cancelling terms in the truncation error, reducing it to

$$\text{error} = O[(\Delta t)^2] + O[(\Delta x)^4] \qquad \ldots\ldots(9)$$

We see from (9) that this provides for a more accurate scheme. An ε , α plot has been done in Figure 12, and as can be seen, this is an improvement for all but the shortest wavelengths. Further the appropriate range of λ has been increased to 0.33.

Scheme 6 is stable for all values of λ , since

$$\lambda \leq \frac{1}{2-4\theta}$$

is automatically satisfied for this particular value of θ .

An alternative arrangement of the scheme can be obtained by removing the terms on the RHS of (4), independent of λ , to the LHS. There results the equivalent scheme:-

$$\tfrac{1}{12}\left\{U_{j+1}^{n+1} - U_{j+1}^{n}\right\} + \tfrac{5}{6}\cdot\left\{U_{j}^{n+1} - U_{j}^{n}\right\} + \tfrac{1}{12}\cdot\left\{U_{j-1}^{n+1} - U_{j-1}^{n}\right\}$$

$$= \tfrac{\lambda}{2}\cdot\left\{(\delta^2 U)_{j}^{n+1} + (\delta^2 U)_{j}^{n}\right\}.$$

Scheme 8.

We consider here the scheme

$$U_j^{n+1} - U_j^{n-1} = 2\lambda\left\{U_{j+1}^n - U_j^{n+1} - U_j^{n-1} + U_{j-1}^n\right\}. \quad \ldots.(10)$$

With a solution of the form

$$U_j^n = \xi^n e^{ikj\Delta x},$$

assumed, we arrive at a quadratic equation in ξ of the form:

$$\xi^2(1+2\lambda) - 4\lambda\cos\alpha\,\xi - (1-2\lambda) = 0. \quad \ldots.(11)$$

The solution to (11) is

$$\xi_{+,-} = \frac{1}{(1+2\lambda)}\cdot\left\{2\lambda\cos\alpha \pm \sqrt{(1-4\lambda^2\sin^2\alpha)}\right\}. \quad \ldots.(12)$$

We note $\xi_{+,-}$ is real for $1 - 4\sin^2\alpha.\lambda^2 > 0$ and complex otherwise. The general solution to (10) is then of the form

$$U_j^n = (A_0\xi_+^n + A_1\xi_-^n)\,e^{ikj\Delta x}$$

where A_0 and A_1 are constants (possibly complex if $\xi_{+,-}$ are). ξ_+ is referred to as the "physical mode", ξ_- the "computational mode". The latter arises because of the nature of the difference scheme.

The error in this scheme is

$$\text{error} = O[(\Delta t)^2] + O[(\Delta x)^2] + O\left[\left(\frac{\Delta t}{\Delta x}\right)^2\right].$$

Here $\Delta t/\Delta x \to 0$ as $\Delta t, \Delta x \to 0$ as a necessary restriction on refining the computational net.

Scheme 8 is always stable for real and complex ξ. For real ξ, $|\xi| < 1$ while for complex ξ, explicitly

$$|\xi_{+,-}| = \sqrt{\frac{2\lambda-1}{2\lambda+1}} < 1.$$

Figure 13 shows some plots of ε (the relative growth factor) against α. For low λ values the curves diverge quite markedly from the ideal case $\varepsilon = 1$, for wavelengths below about $3.5\Delta x$. Associated with these physical modes are quite large computational modes which could prove disastrous for the shorter wavelength features. As λ is increased beyond the value 0.5, complex modes appear and the curves no longer remain simple. These cases introduce phase changes in the original harmonic mode which would lead to distortion in the numerical representation of wavelike disturbances.

$\lambda = 0.5$ is the dividing case between real and complex values for ξ. For $0 \leq \alpha \leq \pi/2$ the "computational mode" curve is the line $\varepsilon = 0$. For $\pi/2 \leq \alpha \leq \pi$, the "physical mode" curve is also the line $\varepsilon = 0$. The other portions are as indicated.

Scheme 10

Another scheme of interest is

$$(1+\theta)\left(U_j^{n+1} - U_j^n\right) - \theta\left(U_j^n - U_j^{n-1}\right) = \lambda\left(\delta^2 U\right)_j^{n+1}, \qquad \ldots(13)$$

where θ is a constant >0.

We try a solution of the form

$$U_j^n = \xi^n e^{ikj\Delta x}.$$

For this to be so, ξ must satisfy the equation

$$(1 + \theta + \lambda x')\xi^2 - (1+2\theta)\xi + \theta = 0, \qquad \ldots(14)$$

where $x' = 4\sin^2\frac{\alpha}{2}$.

The solution to (14) is

$$\xi_{+,-} = \frac{(1+2\theta) \pm \sqrt{(1 - 4\theta\lambda x')}}{2(1+\theta+\lambda x')} \qquad \ldots(15)$$

Again, because of the nature of the numerical scheme, we obtain two values for ξ. The 'plus' sign in (15) gives the "physical mode", and the 'minus' sign the "computational mode". The growth factor ξ, unlike in schems 8, is now a function of a parameter θ as well.

Stability

The above solution is stable provided

$$|\xi_{+,-}| < 1 \qquad \ldots.(16)$$

For real roots (16) is clearly true. The roots $\xi_{+,-}$ are complex when $4\theta\lambda x' > 1$. In this case

$$|\xi_{+,-}|^2 = \frac{\theta}{(1+\theta+\lambda x')}, \qquad \ldots.(17)$$

which is again less than one.

Figures 14-18 display ε , α plots for θ ranging from 0.1 to 0,5 in steps of 0.1. The appropriate values of λ at which complex growth factors arise are given. For θ = 0.1 the complex values lie well away from the line ε = 1 and are not included. As θ is increased the triple points (where the complex and real modes meet) tend to move downwards and to the left, accompanied by a general flattening of the curves.

For wavelike features, only the longer wavelengths appear to be handled well. For the shorter disturbances phase changes are evident resulting from the complex nature of the growth factor ξ .

For equation (13), the truncation error appears to be of the order

$$O[(\Delta t)] + O[(\Delta x)^2].$$

Scheme 11

This is just a special case of scheme 10 when the parameter θ takes the value

$$\theta = \frac{1}{2} + \frac{1}{12\lambda} . \qquad \ldots. (18)$$

This has the effect of cancelling terms in the truncation error reducing it to

$$O[(\Delta t)^2] + O[(\Delta x)^4],$$

thus increasing the accuracy of the numerical scheme.

Complex growth factors exist for all values of λ greater than zero.

Again, only long-wave features are handled well for this scheme. An ε, α plot exhibiting the behaviour of the growth factor is shown in Figure 19.

Scheme 13

The scheme considered here is the rather complicated one:

$$\frac{1}{12}\cdot\left\{\frac{3}{2}U_{j+1}^{n+1} - 2U_{j+1}^{n} + \frac{1}{2}U_{j+1}^{n-1}\right\} + \frac{5}{6}\cdot\left\{\frac{3}{2}U_{j}^{n+1} - 2U_{j}^{n} + \frac{1}{2}U_{j}^{n-1}\right\}$$
$$+ \frac{1}{12}\cdot\left\{\frac{3}{2}U_{j-1}^{n+1} - 2U_{j-1}^{n} + \frac{1}{2}U_{j-1}^{n-1}\right\} = \lambda\left(\delta^2 U\right)_j^{n+1} \qquad \ldots\ldots(19)$$

With a solution of the form

$$U_j^n = \xi^n e^{ikj\Delta x},$$

assumed, ξ must satisfy the quadratic equation

$$(3\cos\alpha + 15 + 12x'\lambda)\xi^2 - (4\cos\alpha + 20)\xi + (5 + \cos\alpha) = 0 \qquad \ldots\ldots(20)$$

Solving for ξ, we have the two solutions

$$\xi_{+,-} = \frac{2(5+\cos\alpha) \pm \sqrt{\{(5+\cos\alpha)^2 - 12x'\lambda(5+\cos\alpha)\}}}{[3(5+\cos\alpha) + 12x'\lambda]}. \qquad \ldots\ldots(21)$$

Stability

For complex roots,

$$|\xi_{+,-}|^2 = \frac{y}{3y + 12x'\lambda} \qquad \ldots\ldots(22)$$

where $y = 5 + \cos\alpha$, and is always less than unity.
For real roots, a little algebra again shows that

$$\xi_{+,-}^2 \leq 1$$

for all α and λ.

Figure 20 displays the appropriate ε, α plot. Only the longer wavelength features are handled well, those at the other end of the spectrum being modified by phase changes due to the complex modes.

The truncation error for this scheme is

$$O[(\Delta t)^2] + O[(\Delta x)^4].$$

Scheme 14 (Saul'ev 1957)

This is the two step scheme:

$$U_j^{n+1} - U_j^n = \lambda \left(U_{j+1}^n - U_j^n - U_j^{n+1} - U_{j-1}^{n+1} \right),$$
$$U_j^{n+2} - U_j^{n+1} = \lambda \left(U_{j+1}^{n+2} - U_j^{n+2} - U_j^{n+1} + U_{j-1}^{n+1} \right),$$

....(23)a-b

so that different schemes are used on alternate time steps. On substituting $\xi^n e^{ikj\Delta x}$ into 23a we have

$$\xi(1+\lambda-\lambda e^{-i\alpha}) = (1-\lambda+\lambda e^{i\alpha}). \quad ....(24)$$

For the second time step we find a growth factor ξ', where

$$\xi'(1+\lambda-\lambda e^{i\alpha}) = (1-\lambda+\lambda e^{-i\alpha}) \quad ....(25)$$

The overall growth factor for the double time step is $\xi\xi'$, where

$$\xi\xi' = \frac{[1-\lambda(1-\cos\alpha)]^2 + \lambda^2 \sin^2\alpha}{[1+\lambda(1-\cos\alpha)]^2 + \lambda^2 \sin^2\alpha} \quad ....(26)$$

after simplification. Since $1-\cos\alpha \geq 0$, $\xi\xi'$ lies in the range $[0, 1]$ and the scheme is unconditionally stable.

The error in the scheme is

$$O[(\Delta t)] + O[(\Delta x)^2],$$

if λ is fixed, otherwise it is

$$O[(\Delta t)^2] + O[(\Delta x)^2] + O[(\tfrac{\Delta t}{\Delta x})^2].$$

Figure 21 shows the plot of $\xi\xi'/e^{-2\lambda\alpha^2}$ against α ; that is, comparing the overall growth factor for the two time steps against the corresponding value in the analytic case. All curves lie in the region $\varepsilon > 1$. For increasing λ they correspondingly diverge more rapidly from $\varepsilon = 1$, but in all cases tend towards $\varepsilon = 1$ for the longer wavelengths modes.

Summary and Conclusion

All the schemes discussed handle the longwave harmonics well. For the shorter wavelength features each scheme exhibits its own characteristics depending on the nature of the differencing scheme employed. In our case where we require a variable vertical grid length in the PBL, we want a scheme that will handle the growth factors of most harmonics while remaining relatively insensitive to the grid length Δz (or $\lambda = \frac{\sigma \Delta t}{(\Delta z)^2}$ for fixed Δt). We also require as large a range of Δz values as possible. Scheme 6 appears to be the best in handling all wavelengths down to about 3 grid lengths with $\lambda \leq 1/3$. Below this discrepancies appear, but then, no scheme handles the very short wavelengths any better.

Appendix

As an example of how to establish the truncation error, we will consider the scheme

$$U_j^{n+1} - U_j^n = \lambda \left\{ U_{j+1}^n - 2U_j^n + U_{j-1}^n \right\}. \qquad \ldots(1)$$

Let $\tilde{U}(x,t)$ be an exact solution of the diffusion equation, with continuous partial derivatives of the orders appearing below. We denote

$\tilde{U}(j\Delta x, n\Delta t)$ by $\tilde{U}_j^n$, and by Taylor's theorem with remainder we have:

$$\tilde{U}_j^{n+1} = \tilde{U}_j^n + (\Delta t)\left(\frac{\partial \tilde{U}}{\partial t}\right)_j^n + \frac{(\Delta t)^2}{2}\cdot\left(\frac{\partial^2 \tilde{U}}{\partial t^2}\right)_j^{n+\theta_1}$$

$$\tilde{U}_{j+1}^n = \tilde{U}_j^n + (\Delta x)\left(\frac{\partial \tilde{U}}{\partial x}\right)_j^n + \frac{(\Delta x)^2}{2}\cdot\left(\frac{\partial^2 \tilde{U}}{\partial x^2}\right)_j^n + \frac{(\Delta x)^3}{6}\cdot\left(\frac{\partial^3 U}{\partial x^3}\right)_j^n + \frac{(\Delta x)^4}{24}\cdot\left(\frac{\partial^4 \tilde{U}}{\partial x^4}\right)_{j+\theta_2}^n,$$

and a similar expansion for $\tilde{U}_{j-1}^n$. θ_1 and θ_2 are numbers between 0 and 1. Since $\tilde{U}$ satisfies the diffusion equation, $\frac{\partial \tilde{U}}{\partial t}$ may be replaced by $\sigma \frac{\partial^2 \tilde{U}}{\partial x^2}$ then, by substituting we find

$$\frac{\tilde{U}_j^{n+1} - \tilde{U}_j^n}{\Delta t} - \frac{\sigma\left(\tilde{U}_{j+1}^n - 2\tilde{U}_j^n + \tilde{U}_{j-1}^n\right)}{(\Delta x)^2}$$

$$= \frac{1}{2}(\Delta t)\left(\frac{\partial^2 \tilde{U}}{\partial t^2}\right)_j^{n+\theta_1} - \frac{\sigma(\Delta x)^2}{24}\left[\left(\frac{\partial^4 \tilde{U}}{\partial x^4}\right)_{j+\theta_2}^n + \left(\frac{\partial^4 \tilde{U}}{\partial x^4}\right)_{j+\theta_3}^n\right].$$

The coefficients of Δt and $(\Delta x)^2$ appearing on the RHS are bounded because of the continuity of the partial derivatives. Expressed symbolically we say the truncation error is;

$$O[(\Delta t)] + O[(\Delta x)^2]$$

Notation

t	time variable
x	space variable
Δt	time interval
Δx	space interval
n	time grid number defined by $n\Delta t = t$.
j	space grid number defined by $j\Delta x = x$.
U_j^n	numerical value of U at the time and space points $n\Delta t$, $j\Delta x$.
δ	space difference defined by $\delta f_j = f_{j+1/2} - f_{j-1/2}$.
k	wave number
α	$= k\Delta x$
λ	$= \sigma \Delta t/(\Delta x)^2$
x'	$= 4. \sin^2\frac{\alpha}{2}$
ξ	growth factor
ξ_+	growth factor for physical mode
ξ_-	growth factor for computational mode

FIG. 1.

SCHEME 5 $\theta = 0$

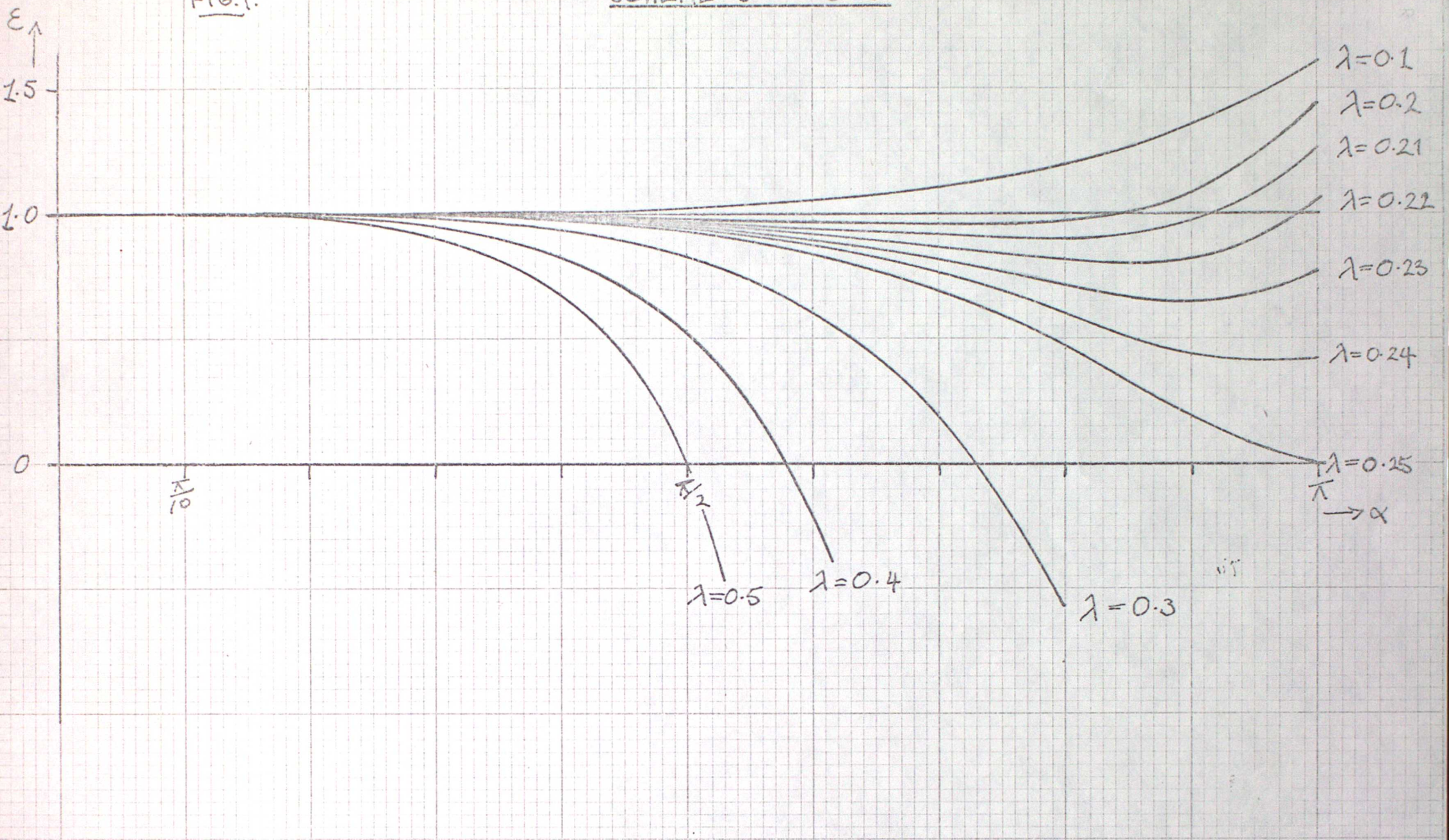

FIG 2.

SCHEME 5 $\theta = 0.1$

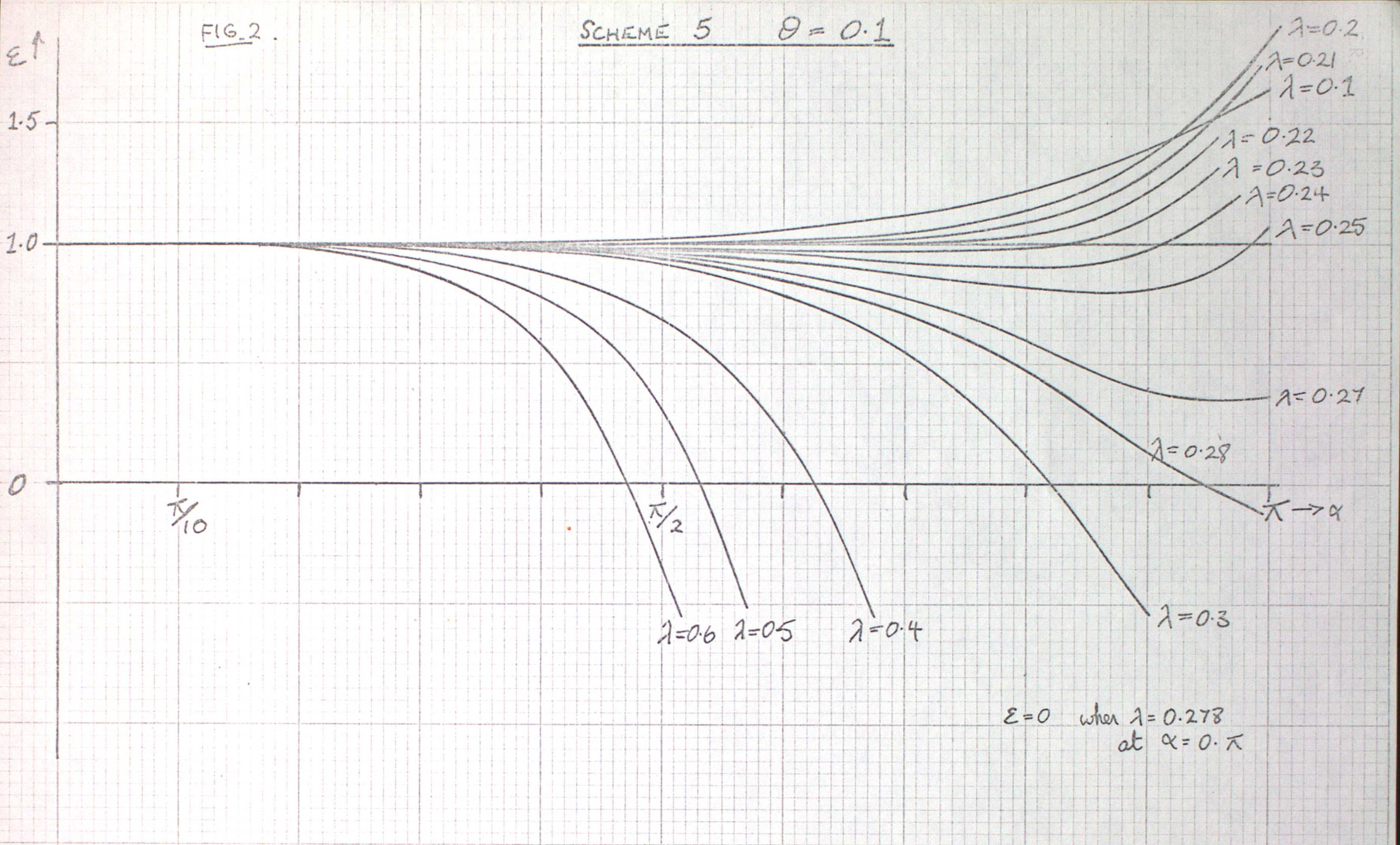

$\varepsilon = 0$ when $\lambda = 0.278$
at $\alpha = 0 \cdot \pi$

FIG. 3

SCHEME 5 $\theta = 0.2$

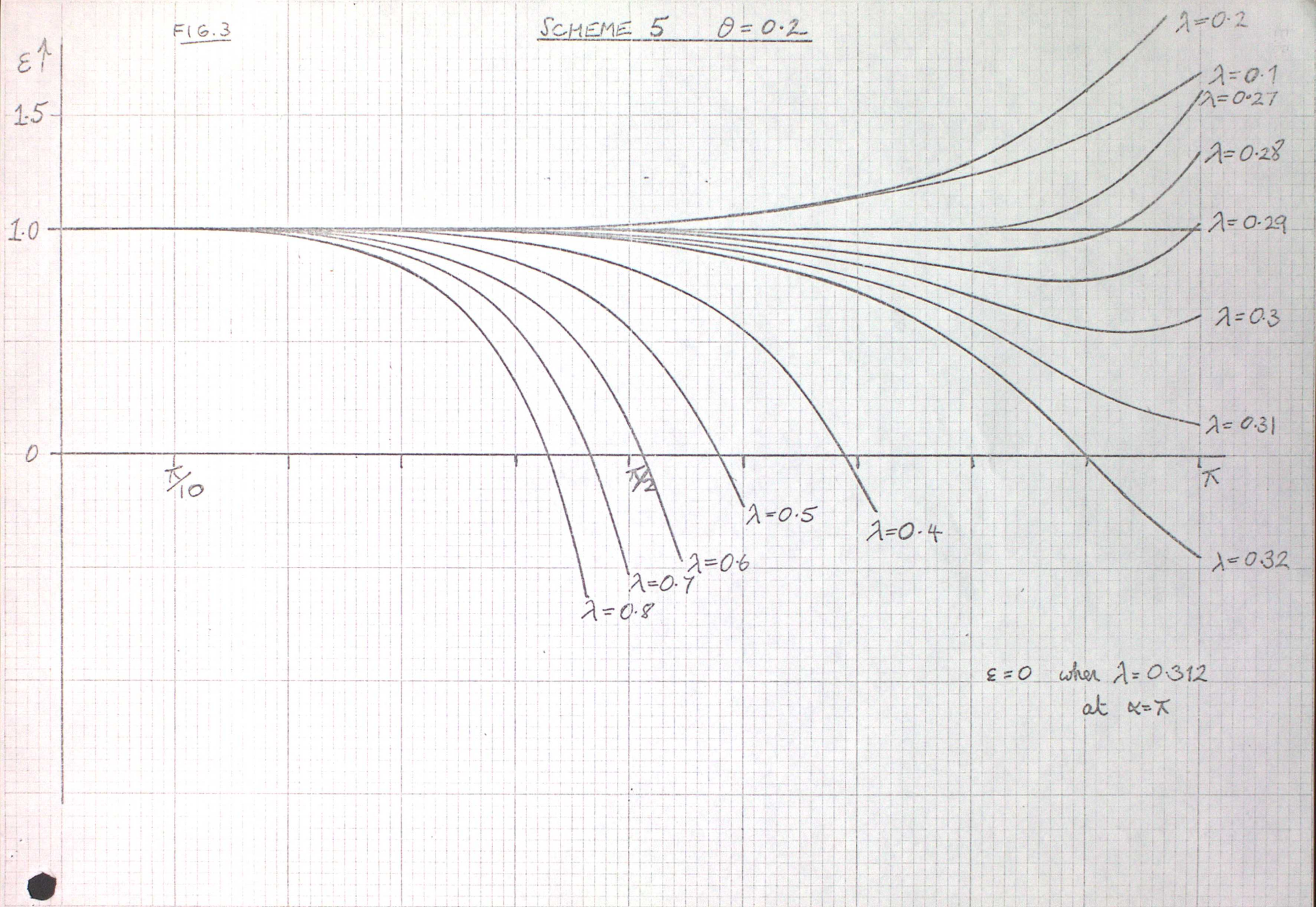

$\varepsilon = 0$ when $\lambda = 0.312$ at $\alpha = \pi$

FIG. 4

SCHEME 5 $\theta = 0.3$

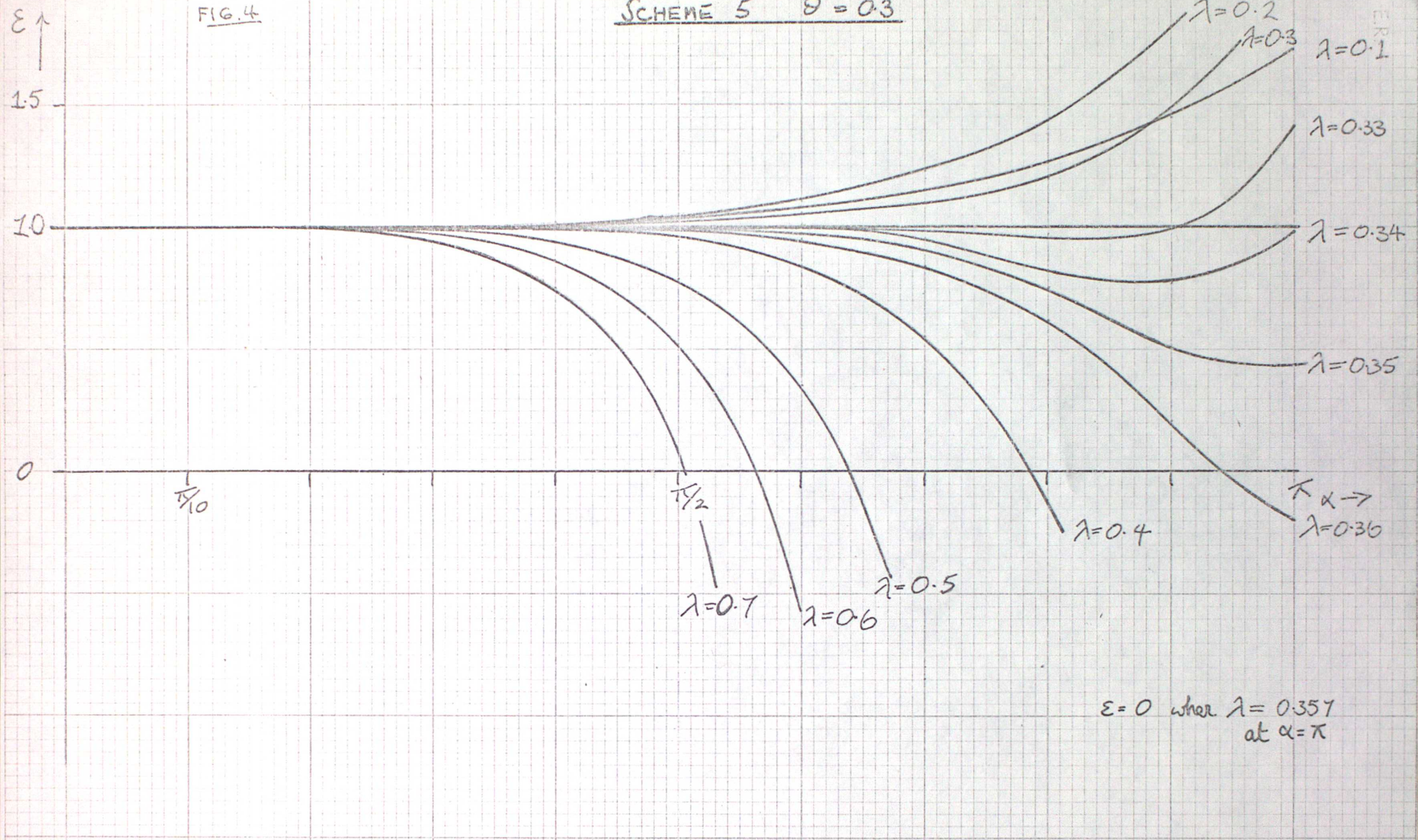

$\varepsilon = 0$ when $\lambda = 0.357$ at $\alpha = \pi$

FIG. 5

SCHEME 5 $\theta = 0.4$

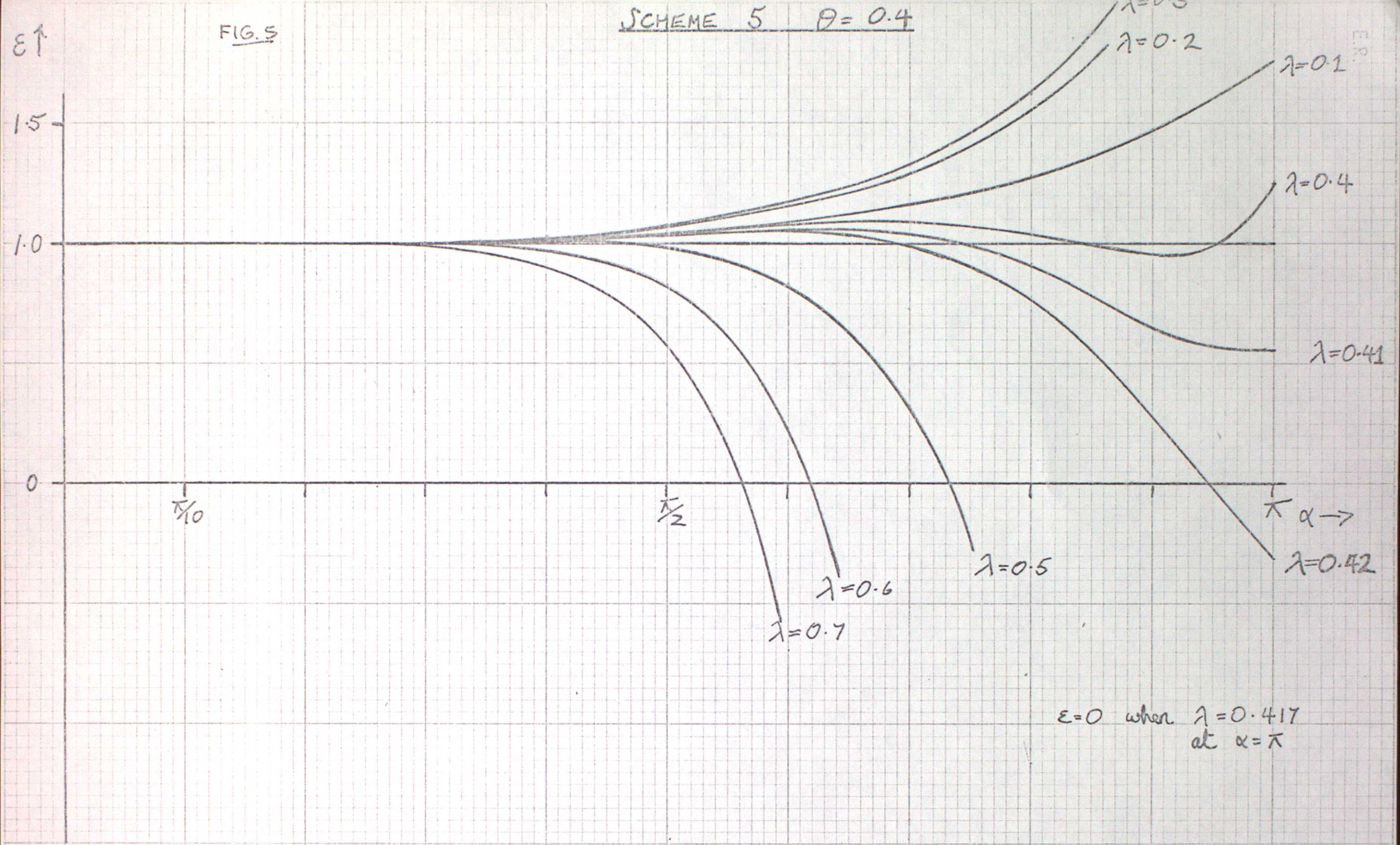

$\varepsilon = 0$ when $\lambda = 0.417$ at $\alpha = \pi$

FIG. 6

SCHEME 5 $\theta = 0.5$

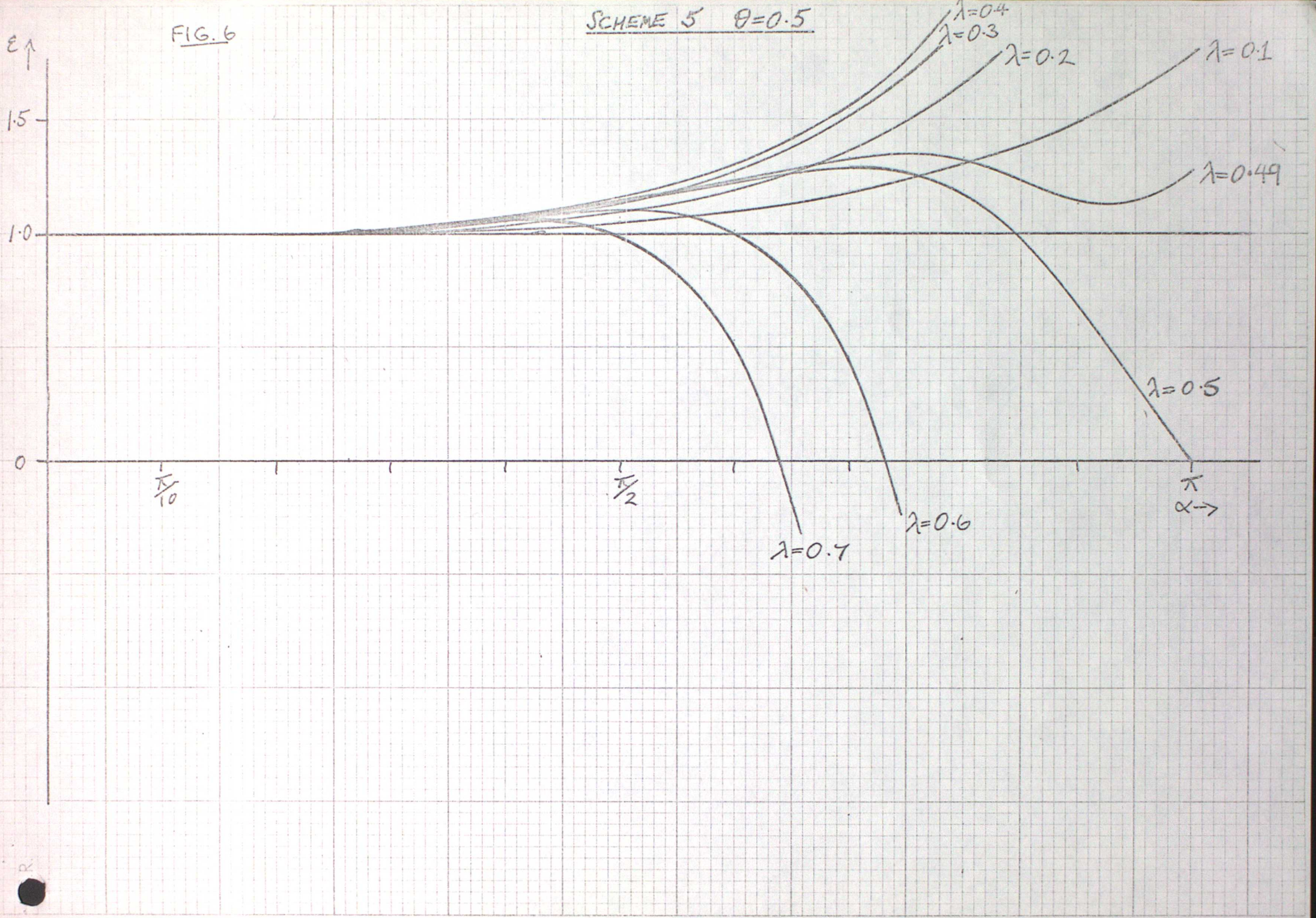

FIG. 7

SCHEME 5 $\theta = 0.6$.

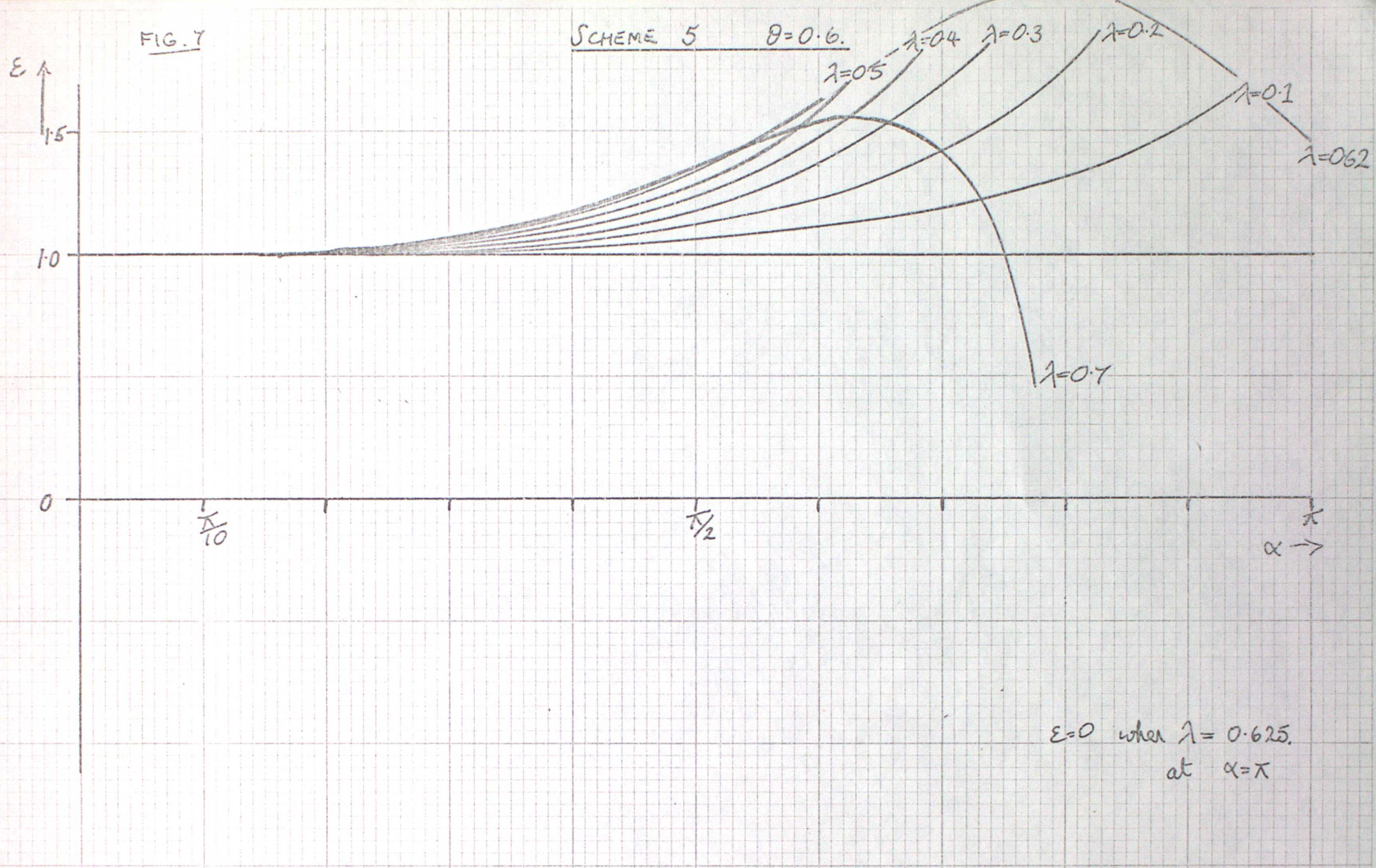

$\varepsilon = 0$ when $\lambda = 0.625$. at $\alpha = \pi$

FIG. 8

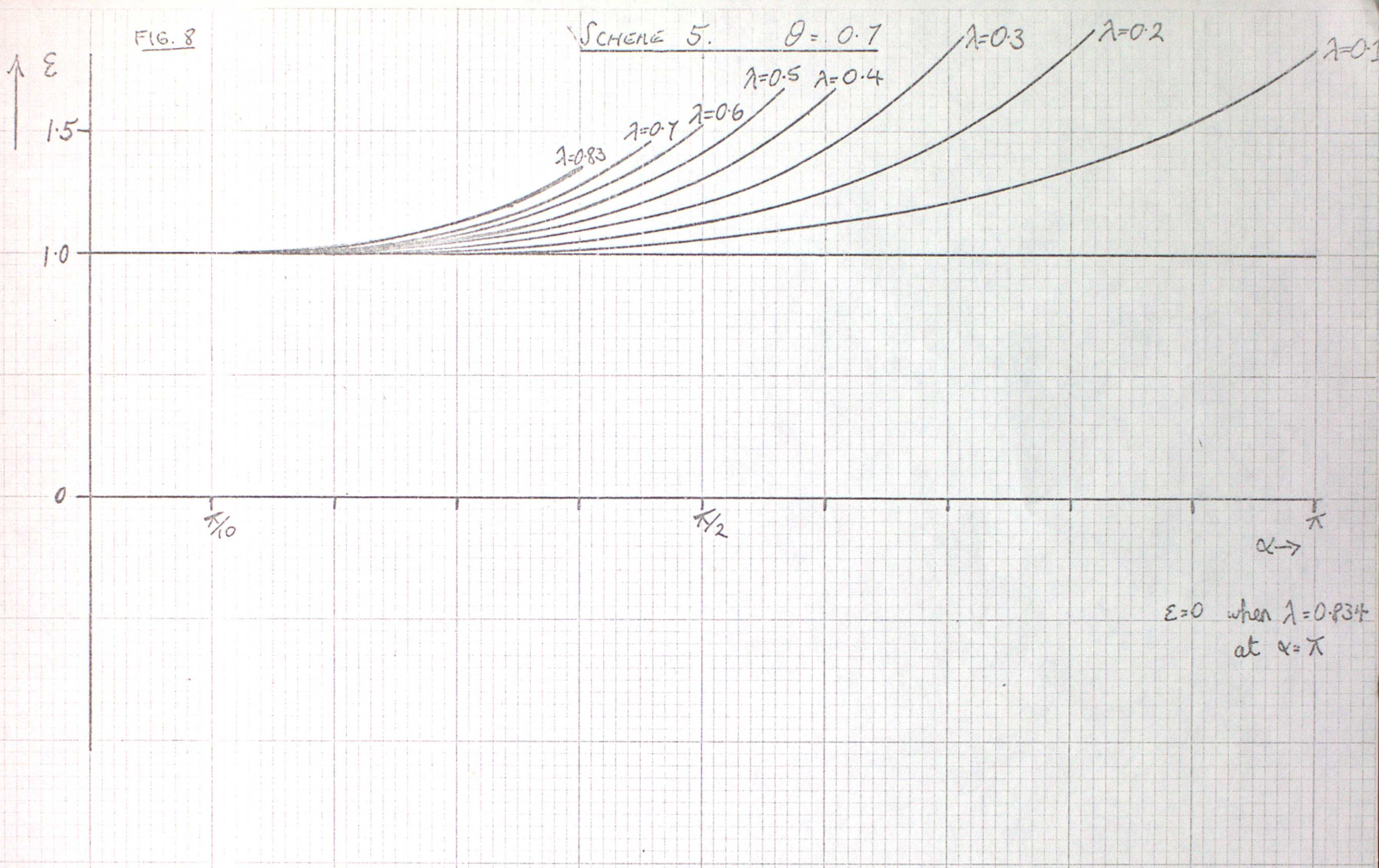

ε=0 when λ=0·834 at α=π

FIG. 9

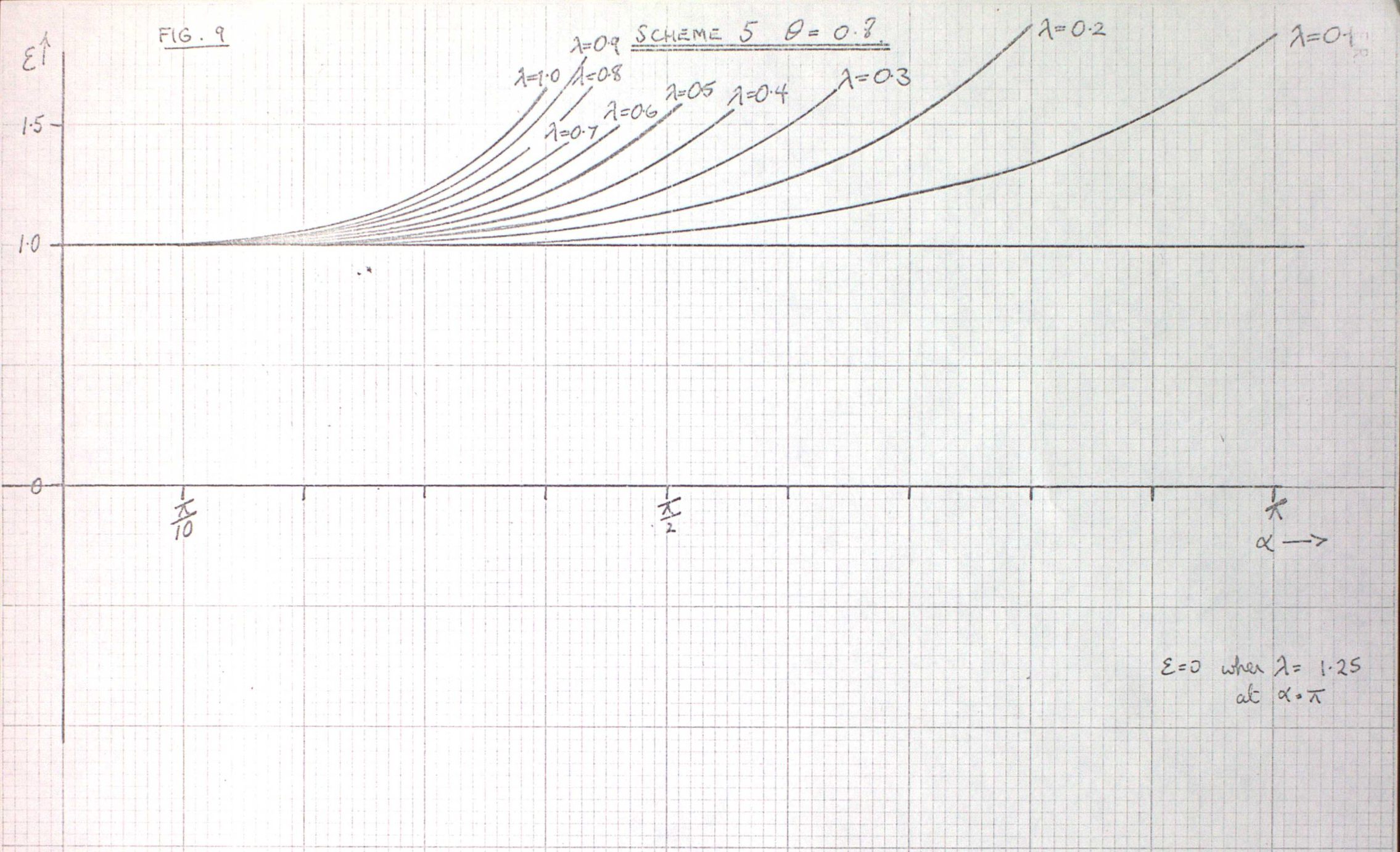

ε=0 when λ = 1·25 at α = π

FIG. 10

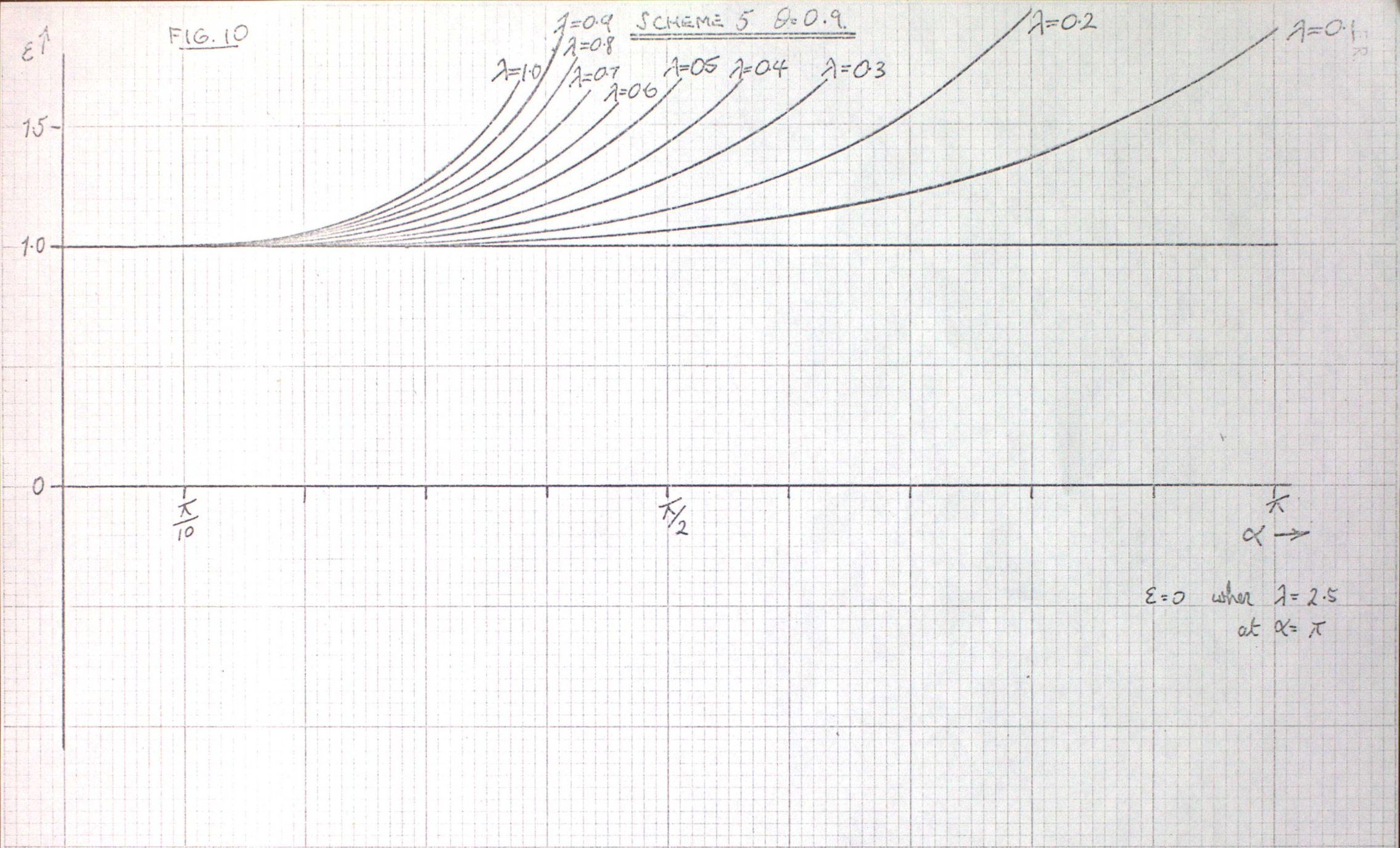

ε=0 when λ=2.5
at α=π

FIG. 11

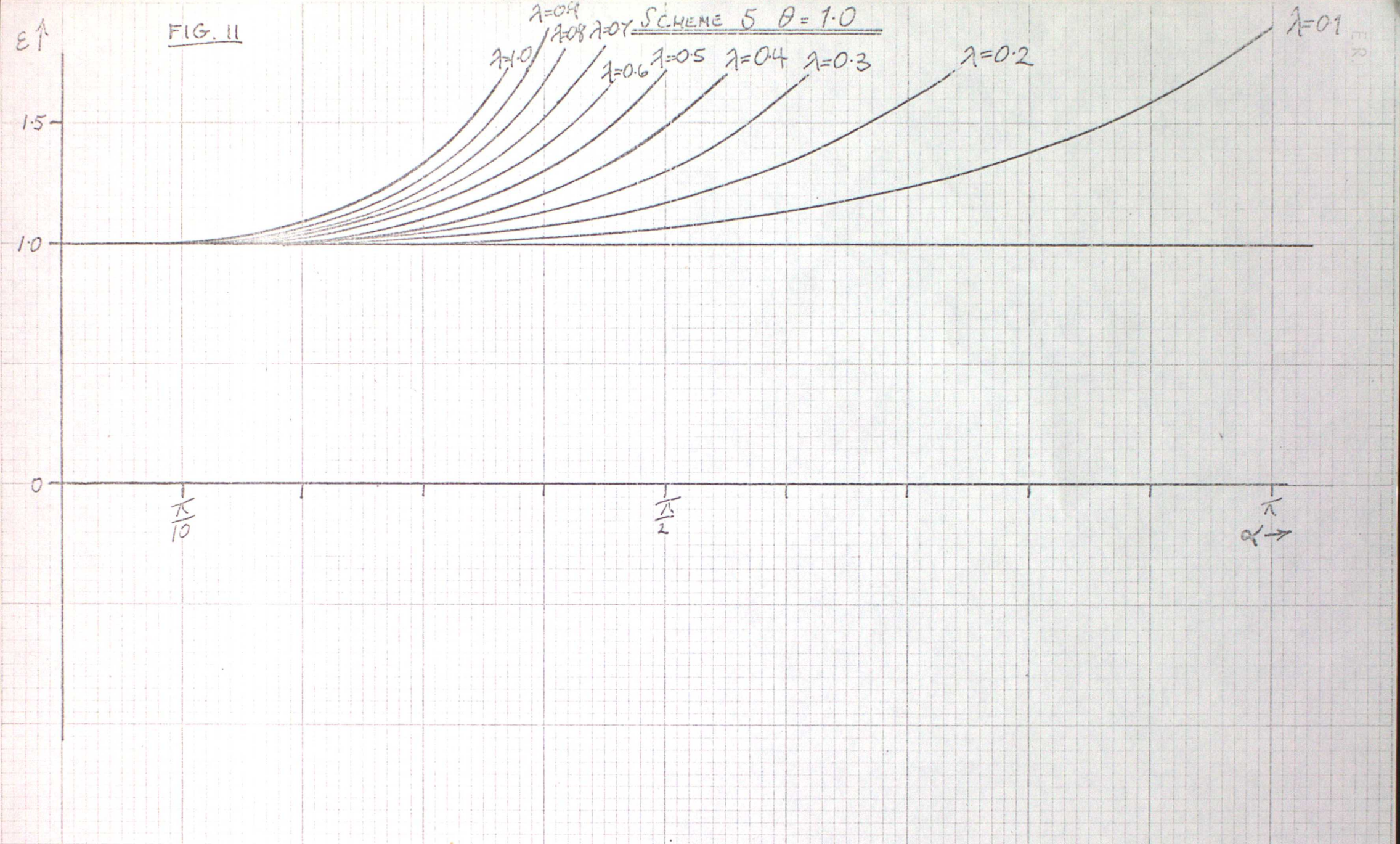
ε ↑
λ=0.9
λ=0.8
λ=0.7
SCHEME 5 θ = 1·0
λ=1·0
λ=0.6
λ=0.5
λ=0.4
λ=0.3
λ=0.2
λ=0·1
1·5
1·0
0
π/10
π/2
π
q →

FIG. 12.

SCHEME 6. $\theta = \frac{1}{2} - \frac{1}{12\lambda}$

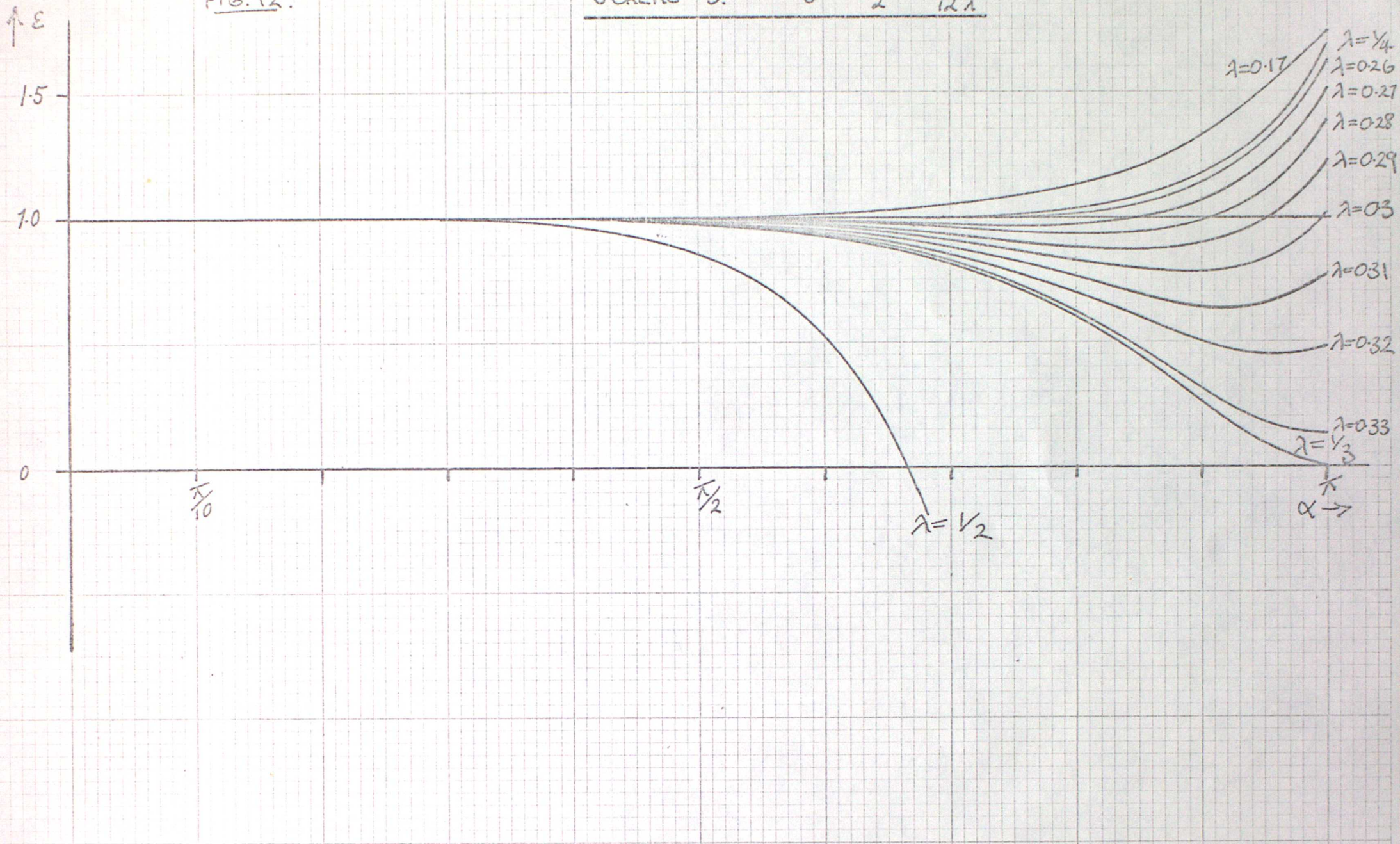

FIG 13

SCHEME 8

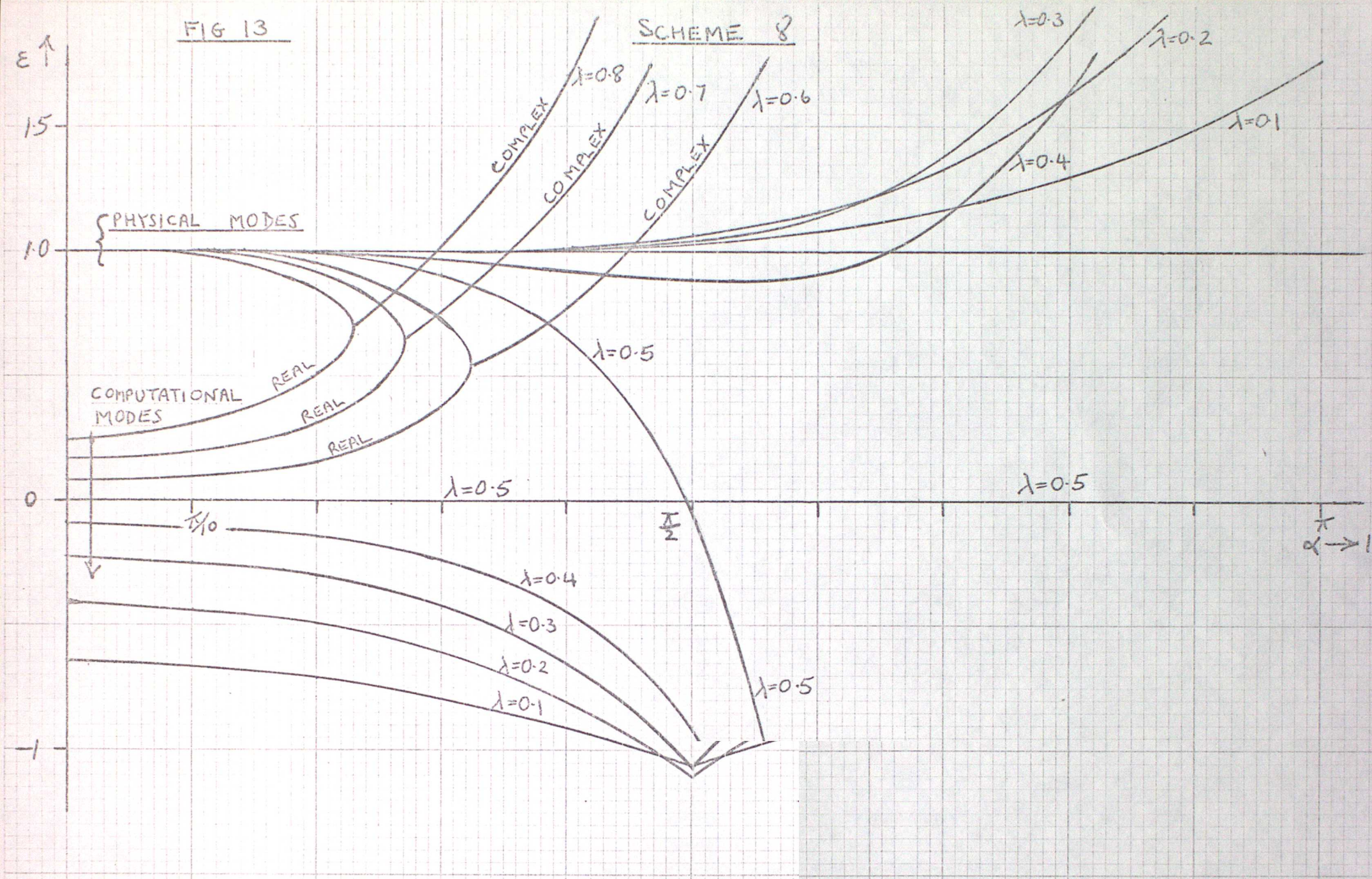

FIG. 14

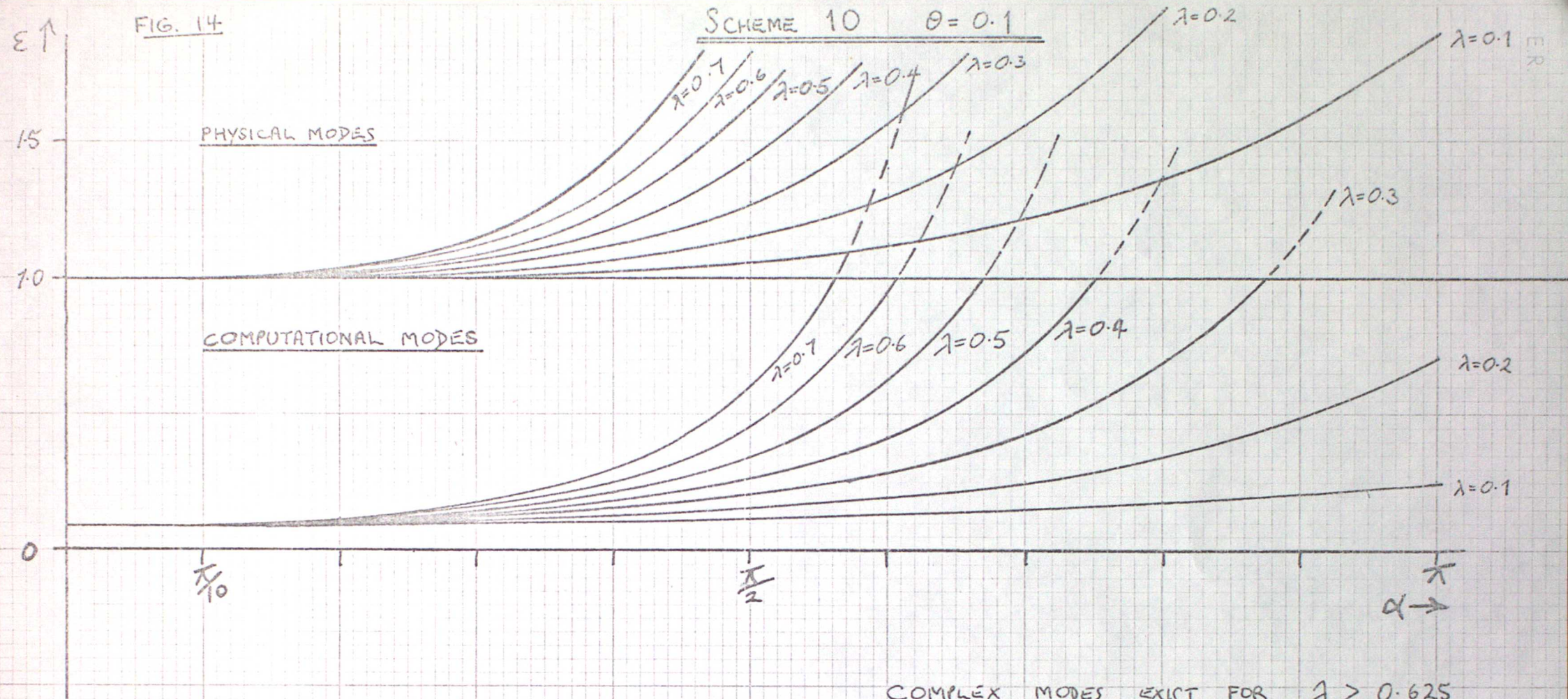

COMPLEX MODES EXIST FOR $\lambda > 0.625$

FIG 15

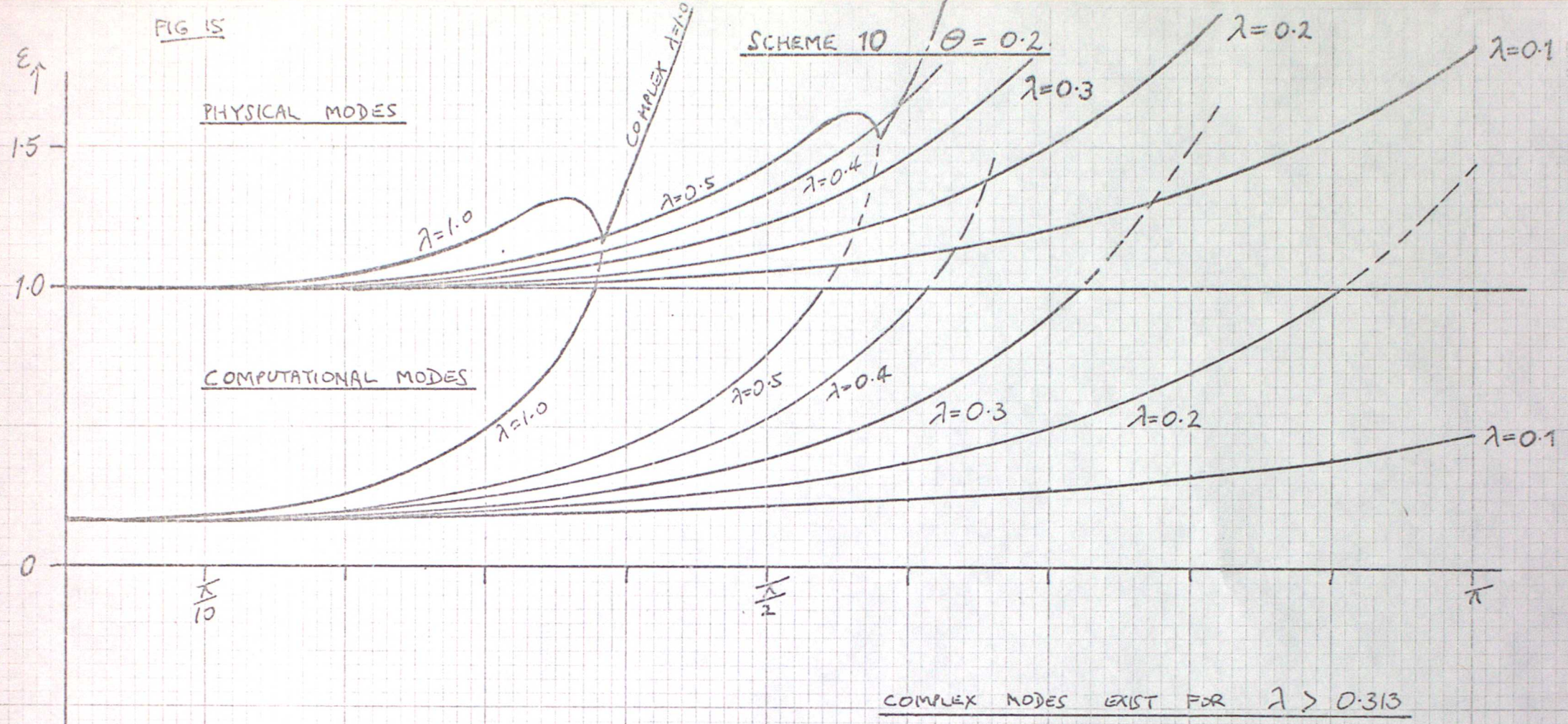

COMPLEX MODES EXIST FOR $\lambda > 0.313$

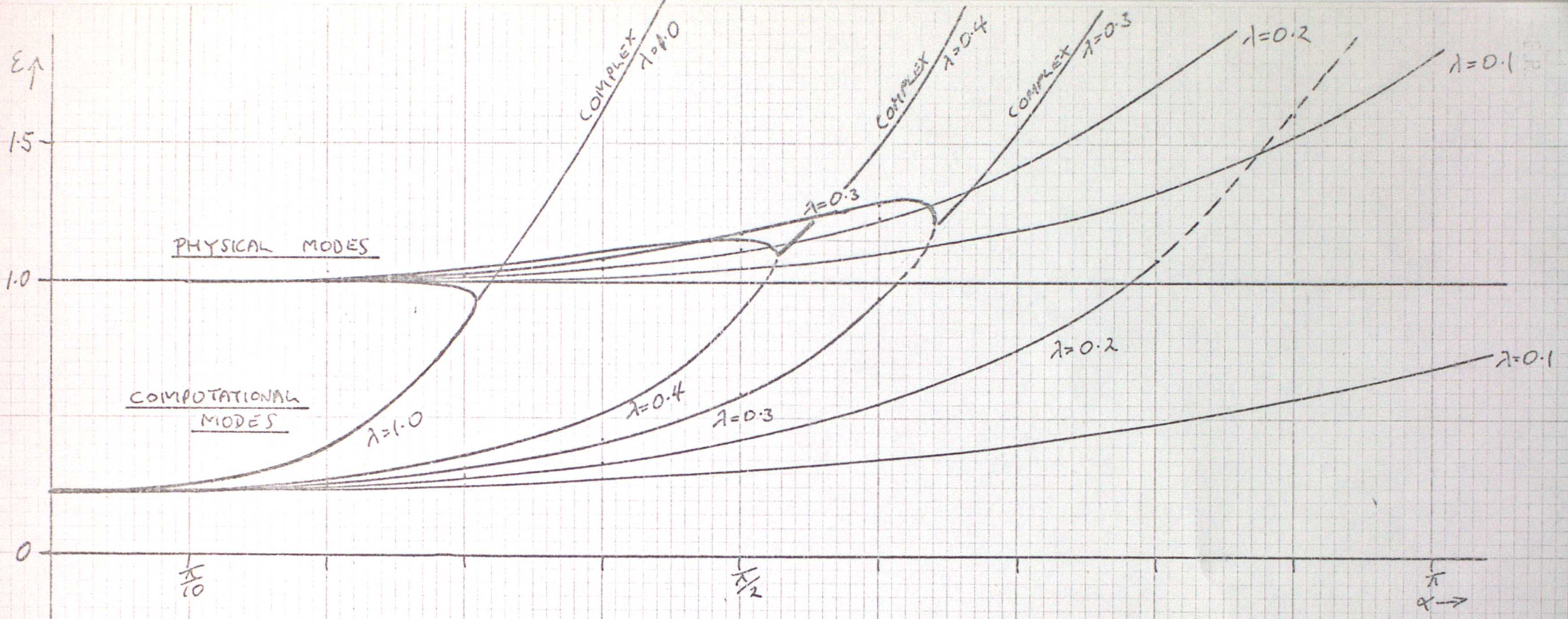

FIG 16. SCHEME 10 $\theta = 0.3$ COMPLEX MODES FOR $\lambda > 0.208$

FIG. 17 SCHEME 10 $\theta = 0.4$

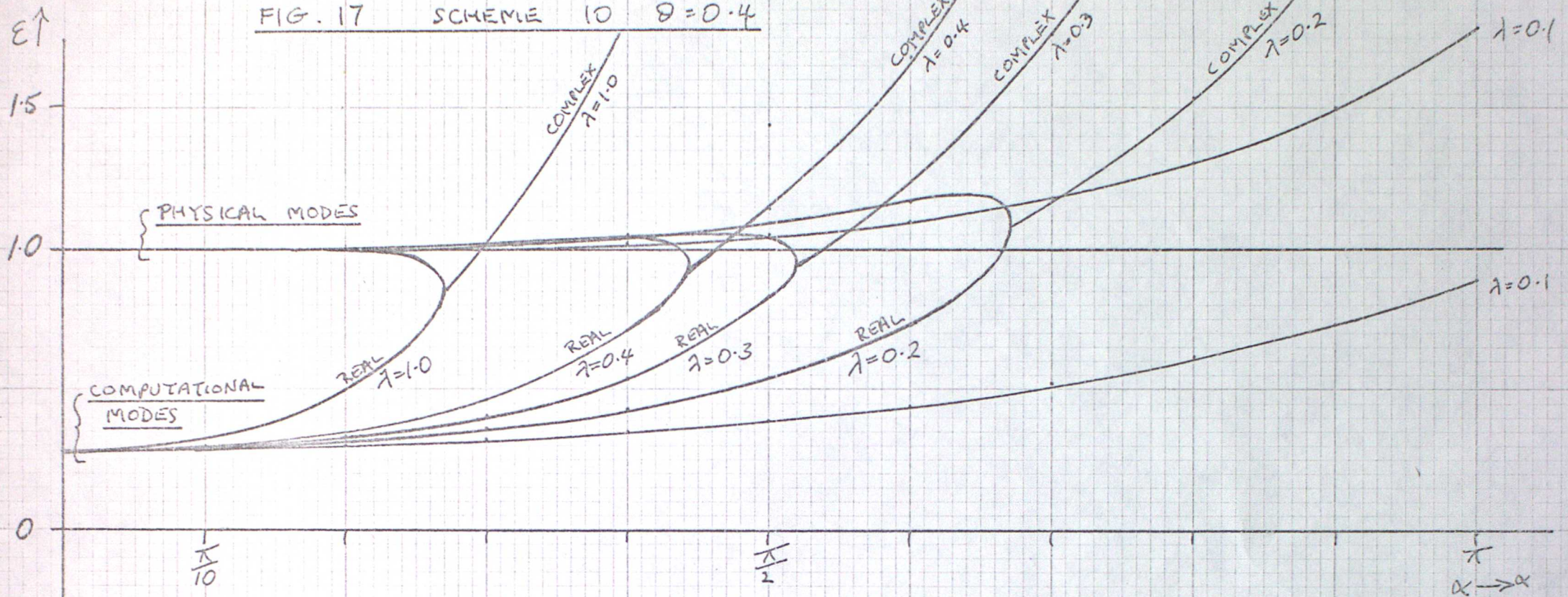

COMPLEX MODES EXIST FOR $\lambda > 0.156$

FIG. 18. SCHEME 10 $\theta = 0.5$

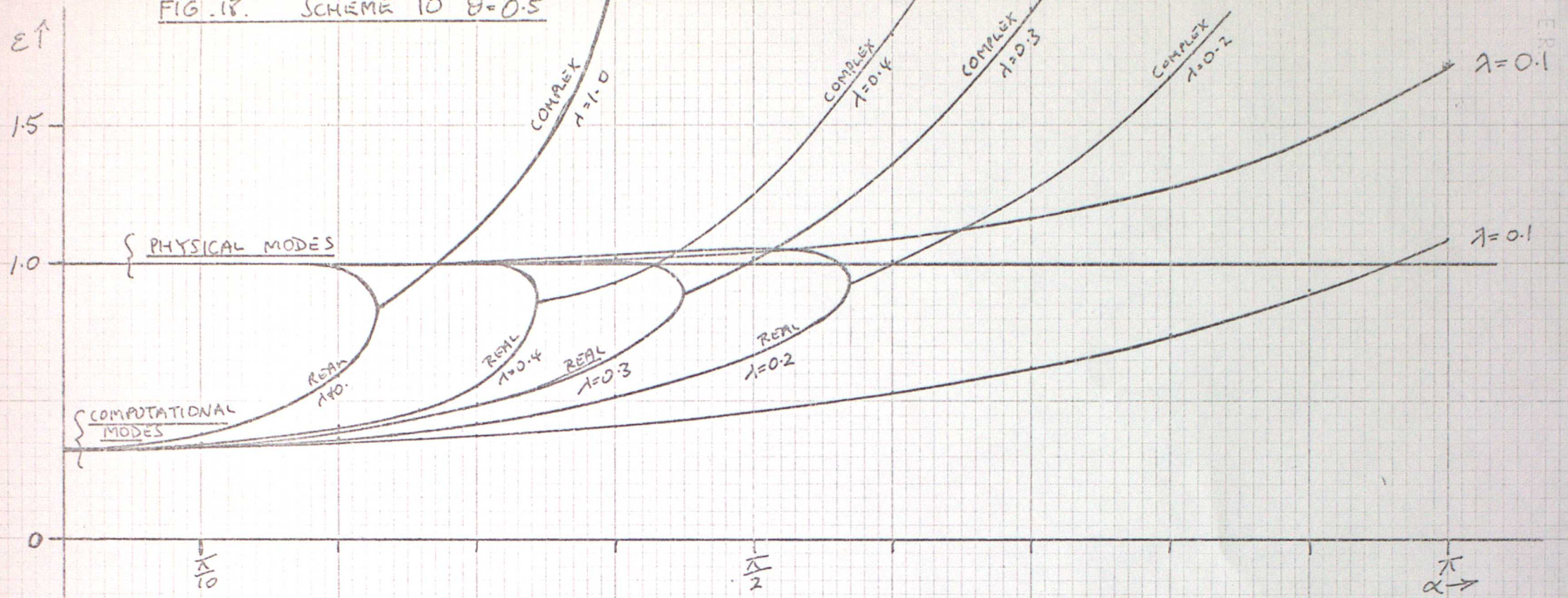

COMPLEX MODES EXIST FOR $\lambda > 0.125$

FIG 19.

SCHEME II : $\theta = \frac{1}{2} + \frac{1}{12\lambda}$

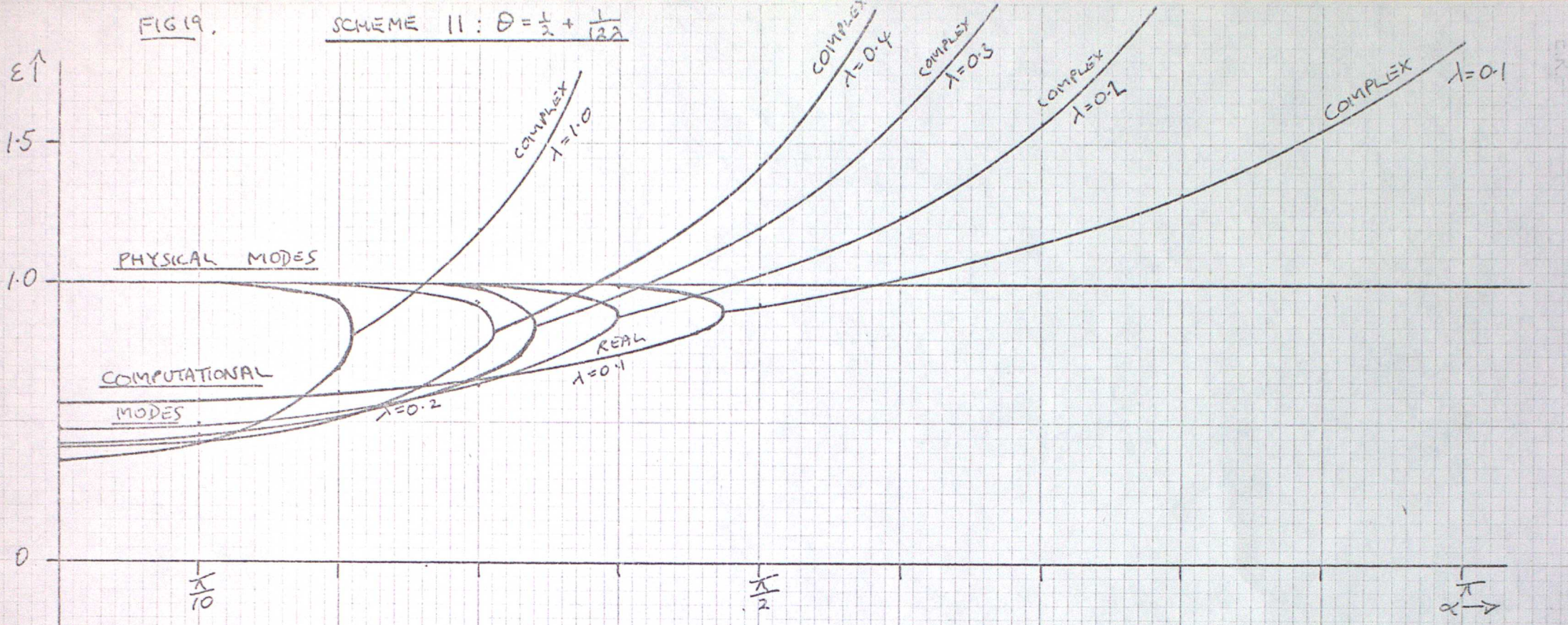

COMPLEX MODES FOR $\lambda > 0$

FIG. 20 SCHEME 13

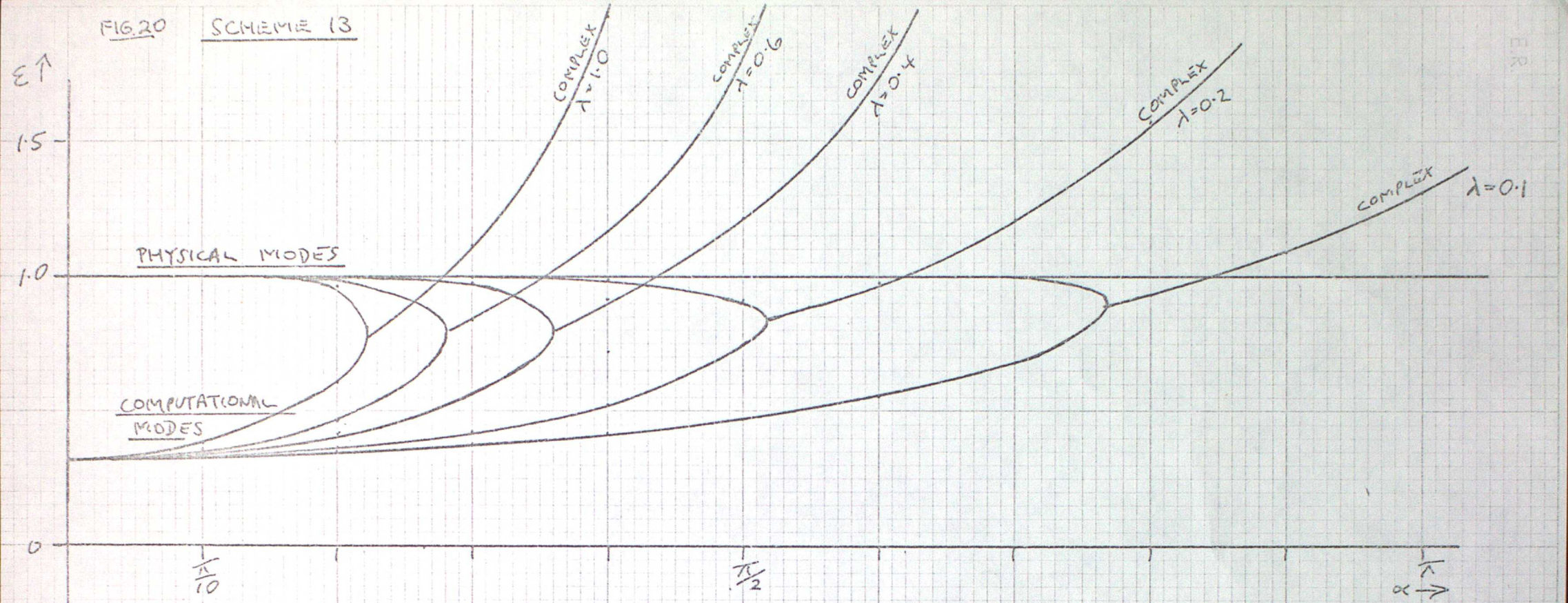

COMPLEX MODES FOR $\lambda > 0.083$

FIG 21

SCHEME 14.